Control of Light-Atom Solitons and Atomic Transport by Optical Vortex Beams Propagating through a Bose-Einstein Condensate

Grant W. Henderson,* Gordon R. M. Robb, Gian-Luca Oppo, and Alison M. Yao
SUPA & Department of Physics, University of Strathclyde, Glasgow, Scotland G4 0NG, United Kingdom

(Received 22 March 2022; accepted 7 July 2022; published 12 August 2022)

We model propagation of far-red-detuned optical vortex beams through a Bose-Einstein condensate using nonlinear Schrödinger and Gross-Pitaevskii equations. We show the formation of coupled light-atomic solitons that rotate azimuthally before moving off tangentially, carrying angular momentum. The number, and velocity, of solitons, depends on the orbital angular momentum of the optical field. Using a Bessel-Gauss beam increases radial confinement so that solitons can rotate with fixed azimuthal velocity. Our model provides a highly controllable method of channeling a BEC and atomic transport.

DOI: 10.1103/PhysRevLett.129.073902

Solitons are localized fields that maintain their spatial profile as they propagate. They have been investigated and realized in fields as diverse as optical fibres [1], hydrodynamics [2], ferromagnetic and antiferromagnetic systems [3], superconductors [4], and even cosmology [5]. Bright [6], dark [7], and lattice [8] solitons have also been observed in Bose-Einstein condensates (BECs). In nonlinear optics, spatial optical solitons [5] arise when the diffraction of a Gaussian beam is carefully balanced by self-focusing due to a Kerr nonlinear medium. However, when the optical field carries orbital angular momentum (OAM) [9], it fragments into solitons, with the number of formed solitons depending, generally, on the OAM index, m [10,11]. This has been confirmed experimentally using hot sodium [12] and rubidium vapors [13] as the Kerr medium. Similar fragmentation has been seen in nonlinear colloidal suspensions [14,15].

In this Letter, we use coupled nonlinear Gross-Pitaevskii and Schrödinger equations to describe the propagation of far-detuned optical fields through a cigar-shaped BEC. We start by confirming that, for weakly repulsive atomic interactions, our model captures the formation of coincident patterns seen in [16] for light that is red detuned with respect to the atoms (so that atoms are attracted to intensity peaks).

We then show that if the light carries OAM, it fragments into solitons during propagation, suggesting that the BEC is behaving like an effective Kerr superfluid. As the atoms are attracted to intensity peaks they are "captured" by the optical solitons, resulting in coupled light-atom solitons. We show that both the optical and atomic solitons carry angular momentum and that the number of solitons formed, and their velocities, is dependent on the OAM of the optical field. The radial spread of the solitons can be reduced by replacing the Laguerre-Gauss optical field with a Bessel-Gauss field.

Our results suggest a highly effective means of channeling large BEC transverse distributions into a given number of tightly confined solitons, presenting a novel method of controllable atomic transport.

A schematic of the proposed setup is shown in Fig. 1(a). A coherent Gaussian beam of waist w_F, typically from a diode laser, is incident on a spatial light modulator (SLM) with an "m"-forked diffraction grating [17] which can convert it to an optical vortex beam carrying OAM of $m\hbar$ per photon [9]. This optical field then propagates through a cigar-shaped BEC moving at velocity v_a, that is suspended by additional horizontal and vertical trapping fields, before being focused onto a detector.

We use a model that describes the mutual spatiotemporal dynamics of an optical field and an ultracold Bose gas of two-level atoms of average velocity v_a equal to the recoil velocity in the mean-field approximation. We consider fields of the form $\Psi(\mathbf{r},t) = \psi(\mathbf{r})\exp[i(k_a z - \omega_a t)]$ and

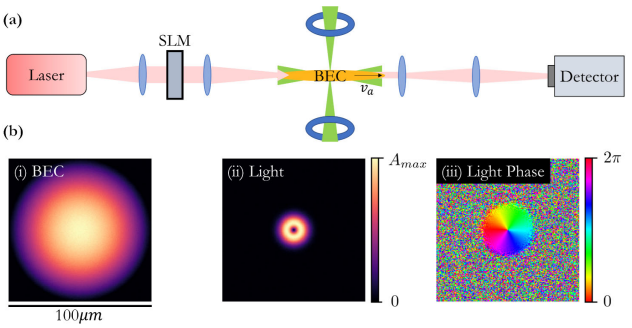

FIG. 1. (a) An input laser beam is incident on an SLM, which can add OAM, before propagating through a cigar-shaped BEC medium moving at velocity v_a, suspended by additional horizontal and vertical trapping fields, to a detector. (b) Transverse cross sections of Thomas-Fermi BEC amplitude with $w_\psi = 50.0\ \mu$m (i), and Laguerre-Gauss optical field amplitude (ii) and phase (iii) with $m = 1$ and $w_F = 10\ \mu$m.

$E(\mathbf{r},t) = F(\mathbf{r})\exp[i(k_L z - \omega_L t)]$, where $\psi(\mathbf{r})$ and $F(\mathbf{r})$ are the slowly varying amplitudes of the BEC wave function and optical field, respectively, with wave numbers $k_a = m_a v_a/\hbar$ and $k_L = 2\pi/\lambda$. Here, m_a is the atomic mass, v_a is the mean or center-of-mass velocity of the atomic beam and, for simplicity, we assume that $k_a \approx k_L$. Such an atomic beam velocity v_a could be applied to the BEC using approaches based around Refs. [18,19].

Our numerical model is similar to that of [16], which describes the coupled propagation dynamics of single frequency paraxial optical and atomic (BEC) beams, but includes terms in L_3 and $\sigma_{\rm sat}$ describing three-body loss and optical saturation, respectively:

$$\partial_\zeta \psi = i\nabla_\perp^2 \psi - i(s|F|^2 + \beta_{\rm col}|\psi|^2 - iL_3|\psi|^4)\psi, \quad (1)$$

$$\partial_\zeta F = i\nabla_\perp^2 F + i\left(\frac{-s|\psi|^2}{1+\sigma_{\rm sat}|F|^2}\right)F. \quad (2)$$

The transverse and longitudinal dimensions are scaled according to $(\xi,\eta) = \sqrt{2}(x,y)/w_F$ and $\zeta = z/(2z_R)$, respectively, where $z_R = \pi w_F^2/\lambda$ is the Rayleigh range.

Equation (1), which describes the evolution of the atomic field, is a reduction of the 3D Gross-Pitaevskii equation to 2D [20]. In Eq. (1) the transverse Laplacian term ($\nabla_\perp^2$) represents the kinetic energy contributions and the $s|F|^2\psi$ term describes light-induced focusing or defocusing due to the dipole interaction. As defined in [16], $\beta_{\rm col}$ is directly proportional to the interatomic scattering length of interactions of ground-state atoms a_{gg}, and thus the term $\beta_{\rm col}|\psi|^2\psi$ describes attractive or repulsive interactions depending on the sign of a_{gg}. Typical scattering parameter values are given in Table I, using atomic parameters from [21]. For clarity we have chosen BEC parameters to match those found for a BEC of weakly *repulsive* cesium atoms ($a_{gg} = 15.7a_0$, with a_0 the Bohr radius), giving $\beta_{\rm col} = 3.5$, but we emphasize that our analysis is applicable over a wide range of scattering lengths, accessible around the Feshbach resonance [22]. As mentioned, we also employ a term $L_3|\psi|^4\psi$ describing three-body loss ($L_3 \approx 10^{-4}$) to arrive at an accurate description of the evolution of the BEC wave function (matter wave) in high-density regimes [23,24]. The selected value of L_3 is in agreement with estimations for cesium [22,25].

TABLE I. Typical ground state scattering parameters a_{gg} of various BEC species with corresponding $\beta_{\rm col}$ values.

Species	a_{gg} [Bohr radius, a_0]	$\beta_{\rm col}$
Lithium	−27.6	−8.22
Sodium	260	117
Rubidium (87)	110	21.6
Cesium	−500 → 500	−110 → 110

Equation (2) is a nonlinear Schrödinger equation describing the propagation of the optical field along the length of the atomic medium. Here, the transverse Laplacian $\nabla_\perp^2$ describes diffraction, the term $s|\psi|^2F$ describes a focusing or defocusing proportional to the atomic density, and $\sigma_{\rm sat}$ describes optical saturation, which is critical to prevent soliton collapse in two transverse dimensions in the case of pure Kerr media [26]. In the Kerr case $\sigma_{\rm sat} = (4P_L)/(3I_{\rm sat}w_F^2)$, where P_L is the power of the incident laser beam and $I_{\rm sat}$ is the saturation intensity [13]. For typical parameter values we find $\sigma_{\rm sat} \approx 10^{-3}$ [10]. Finally, we note that higher order terms corresponding to dipole-dipole forces have been neglected since they only marginally affect the system dynamics and do not alter any of the results presented here.

In both (1) and (2) the parameter $s = \pm 1$ provides a control for the nature of the BEC-optical field dipole coupling. For $s = +1$, the optical field is blue detuned, and the BEC can be described as "dark seeking" with relation to the optical field. For $s = -1$, the optical field is red detuned, and the BEC can be described as "light seeking," and behaves like a self-focusing medium [16]. We numerically integrate Eqs. (1) and (2) using a split-step Fourier method, and include noise at 1% of the amplitude on the initial fields.

The initial wave function of the BEC is a Thomas-Fermi (TF) distribution of amplitude A_ψ and transverse width w_ψ with any negative values set to zero:

$$\psi[r,\zeta(0)] = A_\psi[1 - (r^2)/2w_\psi^2], \quad (3)$$

with $r = \sqrt{(\xi^2+\eta^2)}$. Here, we choose $w_\psi = 50.0\ \mu$m, corresponding to an experimentally realizable BEC with a transverse diameter of 100 μm, and we assume a longitudinal length of around 2 mm [27,28]. We choose a TF distribution to match typical experimental BEC distributions [29], but this specific shape of atomic distribution is not critical, with simply a requirement of a broad enough distribution of BEC atoms with respect to the initial optical field for the dynamics we report to occur. We consider an optical field with wavelength $\lambda = 720$ nm and initial Laguerre-Gaussian profile of amplitude A_F and OAM m at the beam waist w_F [30]:

$$F[r,\varphi,\zeta(0)] = A_F \mathrm{LG}_0^m(r,\varphi)/\max|\mathrm{LG}_0^m|, \quad (4)$$

$$\text{where } \mathrm{LG}_0^m(r,\varphi) = r^{|m|}e^{-(r^2/2)}e^{im\varphi}. \quad (5)$$

Figure 1(b) shows transverse cross sections of typical initial fields ($\zeta = 0$). Panel (i) shows the amplitude of the Thomas-Fermi BEC with $w_\psi = 50.0\ \mu$m. Panels (ii) and (iii) show the amplitude and phase, respectively, of a Laguerre-Gauss optical field with $m = 1$ and beam waist $w_F = 10\ \mu$m chosen so that the beam propagates for several Rayleigh ranges inside the atomic medium ($z_R \approx 0.44$ mm).

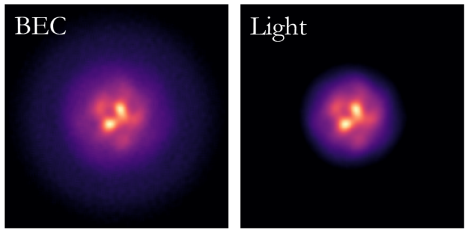

FIG. 2. Coincident pattern formation in both BEC and optical fields for Gaussian input profiles as in Ref. [16]. Transverse scales as in Fig. 1. Parameters: $\beta_{\rm col} = 3.5$, $L_3 = 0.000\,22$, $s = -1$, $w_F = 50$ μm, $A_F = 6$, $w_\psi = 50$ μm, $A_\psi = 6$.

We start by confirming that our model accurately reproduces the results shown in [16,31] for the red-detuned case, $s = -1$. To maximize the area in which the patterns can form, the initial optical field is a Gaussian ($m = 0$) with the same beam waist, $w_F = 50$ μm, as the BEC. The normalized field amplitudes are $A_F = 6$ and $A_\psi = 6$, corresponding to input powers on the order of milliwatt and a total atom number of $\sim 10^5$, respectively. Figure 2 shows the expected formation of *coincident* filament structures at $\zeta = z_R$ arising from a modulational instability due to the dipole interactions between the coupled BEC (left) and optical (right) fields [16]. Soon after the formation of filaments one observes on-axis collapse in both fields as the focusing nonlinearities overwhelm the system dynamics, akin to the BEC collapse experimentally studied in [32]. Although outside the scope of this Letter, our model also confirms similar results seen in 1D [33] that show that on-axis collapse can be avoided when the amplitude of the BEC is significantly different to that of the optical field. In that case the dominant dynamics are linear rather than the highly nonlinear dynamics which we report here, with the optical field acting more as a potential on the BEC rather than a coupled field.

We now consider the effect of adding OAM to the optical beam. With respect to our previous initial conditions, the main difference is that the optical field now has a $0 \to 2m\pi$ azimuthal phase and the corresponding on-axis vortex produces a ringlike intensity profile, as shown in Fig. 1(b) for $m = 1$. We use $A_F = A_\psi = 9.5$, and choose $w_F = 10$ μm so that the beam propagates for several Rayleigh ranges inside the atomic medium ($z_R \approx 0.44$ mm), but emphasize that similar behavior is obtained over a wide range of initial conditions.

Figure 3 shows the resultant optical and atomic fields after numerical integration of (1)–(2) with optical beams carrying OAM of $m = -1$, 1, 2, and 3. We find that adding OAM has a profound effect on the dynamics: the light-seeking atoms now move radially toward the optical ring after which the dynamics of the BEC is closely coupled to that of the light and both fields start to form distinct solitons rather than narrow filaments, in spite of repulsive BEC interactions. Although both atomic density and light

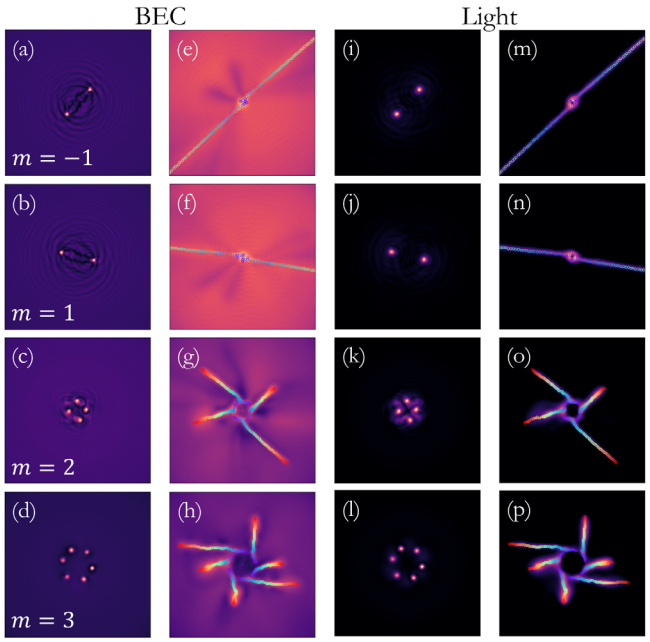

FIG. 3. Panels (a)–(d) and (i)–(l): transverse amplitude cross section of BEC and optical fields, respectively, for $m = -1$, 1, 2, 3 (top to bottom) at $\zeta = z_R$. Panels (e)–(h) and (m)–(p): superimposed images of transverse BEC and optical amplitude distributions, respectively, $\zeta = 0.5 \to 4z_R$. Parameters as in Fig. 2, with $w_F = 10$ μm, $A_F = 9.5$, $A_\psi = 9.5$.

intensity increase significantly within these peaks, there is no collapse of the wave function even with negligible three-body loss. Moreover, we have verified that ring-shaped optical intensity profiles *without* the optical vortex do undergo collapse. Panels (a)–(d) and (i)–(l) show the formation of these $2|m|$ BEC and optical soliton peaks, respectively, at $\zeta = z_R$.

Once the atoms have moved to the ring we see two distinct regimes of atomic motion, both depending on the OAM, m, of the optical field. In the first regime, the OAM leads to an azimuthal motion of the atomic peaks around the ring, analogous to persistent currents [34]. We find that the angular velocity of the solitons is inversely proportional to m^2 and that, in general, this "atomic current" lasts for around $0.75z_R$. This suggests a means of realizing atomic currents within a BEC over a wide range of longitudinal propagation distances as determined by the optical Rayleigh range.

The atoms then enter a second regime where diffractive dynamics begins to dominate and the peaks are ejected tangentially to the ring, thus carrying away the angular momentum. This is demonstrated in panels (e)–(h) and (m)–(p) by overlaying a succession of transverse amplitude distributions from $\zeta = 0.5z_R$ to $4z_R$. We superimpose rainbow contours to highlight the propagation distance (blue at $\zeta = 0.5z_R$, red at $\zeta = 4z_R$). We find that the solitons move with a constant transverse velocity that is inversely proportional to m. This is particularly evident for

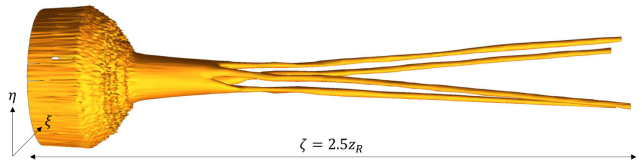

FIG. 4. Three-dimensional BEC distribution for the $m = 2$ case of Fig. 3, $\zeta = 0 \rightarrow 2.5z_R$. Transverse scales as in Fig. 1. Parameters as in Fig. 3.

the $m = -1$ and $m = 1$ cases where the solitons move in opposite directions and agrees very well with previous studies of fragmentation of OAM beams propagating in Kerr self-focusing media, predicted in [10,11] and more recently demonstrated experimentally in [13]. The number of atomic solitons formed, and their tangential velocity (again scaled by the Rayleigh range), depends on the OAM of the optical input field meaning that it is possible to realize these controllable atomic transport dynamics across a wide range of longitudinal propagation distances, transverse field sizes, and OAM values.

The overall behavior of the system is summarized well in Fig. 4, which shows in 3D the redistribution of the atoms as the far-red-detuned light propagates along the length of the BEC for the case of $m = 2$. The atoms, initially in a TF distribution, are focused onto a ring before splitting into four channels that *twist* as they propagate.

We find that the coupled off-axis soliton formation process is robust across a wide range of OAM values, initial field amplitudes, beam sizes, and BEC scattering parameters for both weakly attractive and repulsive interactions in the range $-20a_0 < a_{gg} < 50a_0$ corresponding to $-4 < \beta_{\mathrm{col}} < 11$. We note that three-body loss contributions are negligible for repulsive scattering, $\beta_{\mathrm{col}} > 0$, but become more important for increasingly attractive scattering interactions. In particular, we find that both optical and atomic solitons propagate tangentially with little change to their shape or amplitude until they reach the transverse limits of the BEC.

We can extend the duration of the azimuthal rotation and decrease the transverse motion of the solitons by replacing the Laguerre-Gauss mode (5) with an equivalent Bessel-Gauss (BG) mode:

$$F_{\mathrm{BG}}(r, \varphi, 0) = J_m(\kappa r) e^{-(r^2/2)} e^{im\varphi}, \tag{6}$$

where J_m represents the mth order Bessel function and we choose κ such that the size of the central ring of the BG mode matches that of the equivalent LG mode. BG beams are solutions to the paraxial wave equation that, by controlling the width of the Gaussian, encompass as limiting cases the diffraction-free Bessel beam and the Gaussian beam [35,36]. Typically, these can be made in the lab by utilizing a circular slit to transform a plane wave [37], or (specifically for a BG setup) by using an axicon lens to focus a Gaussian beam [38].

As before, we find that $2|m|$ solitons form. For the weakly *repulsive* scattering regime ($\beta_{\mathrm{col}} = 3.5$), the diffraction-less nature of the BG beams increases the length that the atoms are confined to the ring to $\approx 1.2z_R$, and decreases the radial spread of the solitons at $4z_R$ by ≈ 1.5 times. If we move to weakly *attractive* interactions ($\beta_{\mathrm{col}} = -1.5$) we find that, for $m = 1, 2$, the solitons rotate azimuthally with constant velocity along the entire length of the atomic medium, thus producing a form of controllable persistent current.

In conclusion, we have demonstrated the formation of *coupled* optical and atomic solitons carrying angular momentum when far-red-detuned light carrying OAM propagates through a BEC. Despite fundamental differences between the coupled BEC-light model and the pure Kerr case, we find that both optical and atomic fields break into $2|m|$ solitons as in the Kerr case [10,11]. These rotate azimuthally around the ring of maximum intensity of the light before breaking away and moving tangentially such that angular momentum is conserved. The number of solitons and their transverse velocity can be controlled by the OAM of the optical beam, with potential applications in atomic transport. By using a Bessel-Gauss beam of equivalent radius and OAM, and moving to weakly attractive interactions we are able to transversely confine the solitons so that they continue to rotate azimuthally for the entire length of the BEC. This has the potential for realising controllable persistent currents in a BEC without the introduction of complex trapping potentials.

The data presented in this publication can be openly accessed through the University of Strathclyde KnowledgeBase [39].

We thank E. Haller for useful discussions. We acknowledge support from EPSRC (EP/R513349/1) via a Doctoral Training Partnership and from the European Training Network ColOpt, which is funded by the European Union (EU) Horizon 2020 program under the Marie Skłodowska-Curie Action, Grant Agreement No. 721465.

*grant.henderson@strath.ac.uk

[1] L. F. Mollenauer, R. H. Stolen, and J. P. Gordon, Experimental Observation of Picosecond Pulse Narrowing and Solitons in Optical Fibers, Phys. Rev. Lett. **45**, 1095 (1980).
[2] Junru Wu, Robert Keolian, and Isadore Rudnick, Observation of a Nonpropagating Hydrodynamic Soliton, Phys. Rev. Lett. **52**, 1421 (1984).
[3] A. M. Kosevich, B. A. Ivanov, and A. S. Kovalev, Magnetic solitons, Phys. Rep. **194**, 117 (1990).
[4] Y. Tanaka, Soliton in Two-Band Superconductor, Phys. Rev. Lett. **88**, 017002 (2001).
[5] Thierry Dauxois, *Physics of Solitons* (Cambridge University Press, Cambridge, England, 2010).

[6] L. Khaykovich, F. Schreck, G. Ferrari, T. Bourdel, J. Cubizolles, L. D. Carr, Y. Castin, and C. Salomon, Formation of a matter-wave bright soliton, Science **296**, 1290 (2002).
[7] J. Denschlag, J. E. Simsarian, D. L. Feder, Charles W. Clark, L. A. Collins, J. Cubizolles, Lu Deng, Edward W. Hagley, Kristian Helmerson, William P. Reinhardt *et al.*, Generating solitons by phase engineering of a Bose-Einstein condensate, Science **287**, 97 (2000).
[8] B. Eiermann, Th. Anker, M. Albiez, M. Taglieber, P. Treutlein, K.-P. Marzlin, and M. K. Oberthaler, Bright Bose-Einstein Gap Solitons of Atoms with Repulsive Interaction, Phys. Rev. Lett. **92**, 230401 (2004).
[9] L. Allen, M. W. Beijersbergen, R. J. C. Spreeuw, and J. P. Woerdman, Orbital angular momentum of light and the transformation of Laguerre-Gaussian laser modes, Phys. Rev. A **45**, 8185 (1992).
[10] W. J. Firth and D. V. Skryabin, Optical Solitons Carrying Orbital Angular Momentum, Phys. Rev. Lett. **79**, 2450 (1997).
[11] Anton S. Desyatnikov and Yuri S. Kivshar, Necklace-Ring Vector Solitons, Phys. Rev. Lett. **87**, 033901 (2001).
[12] Matthew S. Bigelow, Petros Zerom, and Robert W. Boyd, Breakup of Ring Beams Carrying Orbital Angular Momentum in Sodium Vapor, Phys. Rev. Lett. **92**, 083902 (2004).
[13] Frédéric Bouchard, Hugo Larocque, Alison M. Yao, Christopher Travis, Israel De Leon, Andrea Rubano, Ebrahim Karimi, Gian-Luca Oppo, and Robert W. Boyd, Polarization Shaping for Control of Nonlinear Propagation, Phys. Rev. Lett. **117**, 233903 (2016).
[14] W. Walasik, S. Z. Silahli, and N. M. Litchinitser, Dynamics of necklace beams in nonlinear colloidal suspensions, Sci. Rep. **7**, 11709 (2017).
[15] Jingbo Sun, Salih Z. Silahli, Wiktor Walasik, Qi Li, Eric Johnson, and Natalia M. Litchinitser, Nanoscale orbital angular momentum beam instabilities in engineered nonlinear colloidal media, Opt. Express **26**, 5118 (2018).
[16] Mark Saffman and Dmitry V. Skryabin, Coupled propagation of light and matter waves: Solitons and transverse instabilities, in *Spatial Solitons*, edited by Stefano Trillo and William Torruellas (Springer, Berlin, Heidelberg, 2001), pp. 433–447.
[17] N. R. Heckenberg, R. McDuff, C. P. Smith, and A. G. White, Generation of optical-phase singularities by computer generated holograms, Opt. Lett. **17**, 221 (1992).
[18] W. Guerin, J.-F. Riou, J. P. Gaebler, V. Josse, P. Bouyer, and A. Aspect, Guided Quasicontinuous Atom Laser, Phys. Rev. Lett. **97**, 200402 (2006).
[19] Immanuel Bloch, Theodor W. Hänsch, and Tilman Esslinger, Atom Laser with a cw Output Coupler, Phys. Rev. Lett. **82**, 3008 (1999).
[20] L. Salasnich, A. Parola, and L. Reatto, Effective wave equations for the dynamics of cigar-shaped and disk-shaped Bose condensates, Phys. Rev. A **65**, 043614 (2002).
[21] D. A. Steck, Alkali D line data, available online at http://steck.us/alkalidata (2022).
[22] Andrea Di Carli, Grant Henderson, Stuart Flannigan, Craig D. Colquhoun, Matthew Mitchell, Gian-Luca Oppo, Andrew J. Daley, Stefan Kuhr, and Elmar Haller, Collisionally Inhomogeneous Bose-Einstein Condensates with a Linear Interaction Gradient, Phys. Rev. Lett. **125**, 183602 (2020).
[23] P. A. Altin, G. R. Dennis, G. D. McDonald, D. Döring, J. E. Debs, J. D. Close, C. M. Savage, and N. P. Robins, Collapse and three-body loss in a ^{85}Rb Bose-Einstein condensate, Phys. Rev. A **84**, 033632 (2011).
[24] P. Köberle, D. Zajec, G. Wunner, and B. A. Malomed, Creating two-dimensional bright solitons in dipolar Bose-Einstein condensates, Phys. Rev. A **85**, 023630 (2012).
[25] Tobias Kraemer, Manfred Mark, Philipp Waldburger, Johann G. Danzl, Cheng Chin, Bastian Engeser, Almar D. Lange, Karl Pilch, Antti Jaakkola, H.-C. Nägerl, and R. Grimm, Evidence for Efimov quantum states in an ultracold gas of caesium atoms, Nature (London) **440**, 315 (2006).
[26] Luc Bergé, Wave collapse in physics: Principles and applications to light and plasma waves, Phys. Rep. **303**, 259 (1998).
[27] A. Di Carli, C. D. Colquhoun, S. Kuhr, and E. Haller, Interferometric measurement of micro-g acceleration with levitated atoms, New J. Phys. **21**, 053028 (2019).
[28] D. S. Petrov, G. V. Shlyapnikov, and J. T. M. Walraven, Phase-Fluctuating 3D Bose-Einstein Condensates in Elongated Traps, Phys. Rev. Lett. **87**, 050404 (2001).
[29] Franco Dalfovo, Stefano Giorgini, Lev P. Pitaevskii, and Sandro Stringari, Theory of Bose-Einstein condensation in trapped gases, Rev. Mod. Phys. **71**, 463 (1999).
[30] Stephen M. Barnett and Roberta Zambrini, Orbital angular momentum of light, in *Quantum Imaging*, edited by Mikhail I. Kolobov (Springer, New York, NY, 2007), pp. 277–311.
[31] M. Saffman, Self-Induced Dipole Force and Filamentation Instability of a Matter Wave, Phys. Rev. Lett. **81**, 65 (1998).
[32] Elizabeth A. Donley, Neil R. Claussen, Simon L. Cornish, Jacob L. Roberts, Eric A. Cornell, and Carl E. Wieman, Dynamics of collapsing and exploding Bose-Einstein condensates, Nature (London) **412**, 295 (2001).
[33] F. Cattani, A. Kim, D. Anderson, and M. Lisak, Co-propagating Bose-Einstein condensates and electromagnetic radiation: Emission of mutually localized structures, Phys. Rev. A **83**, 013608 (2011).
[34] J. File and R. G. Mills, Observation of Persistent Current in a Superconducting Solenoid, Phys. Rev. Lett. **10**, 93 (1963).
[35] F. Gori, G. Guattari, and C. Padovani, Bessel-Gauss beams, Opt. Commun. **64**, 491 (1987).
[36] D. McGloin and K. Dholakia, Bessel beams: Diffraction in a new light, Contemp. Phys. **46**, 15 (2005).
[37] J. Durnin, J. J. Miceli, and J. H. Eberly, Diffraction-Free Beams, Phys. Rev. Lett. **58**, 1499 (1987).
[38] V. Garcés-Chávez, David McGloin, H. Melville, Wilson Sibbett, and Kishan Dholakia, Simultaneous micromanipulation in multiple planes using a self-reconstructing light beam, Nature (London) **419**, 145 (2002).
[39] G. W. Henderson, G. R. M. Robb, G.-L. Oppo, and A. M. Yao, Data for: "Control of Light-Atom Solitons and Atomic Transport by Optical Vortex Beams Propagating through a Bose-Einstein Condensate", University of Strathclyde KnowledgeBase, 10.15129/35149510-7fa5-46b8-80d9-233dbb582a28.